Neuron, Vol. 23, 399–409, June, 1999, Copyright ©1999 by Cell Press

Released Fraction and Total Size of a Pool of Immediately Available Transmitter Quanta at a Calyx Synapse

Ralf Schneggenburger,* Alexander C. Meyer, and Erwin Neher
Max-Planck-Institut für biophysikalische Chemie
Abteilung Membranbiophysik
Am Fassberg 11
D-37077 Göttingen
Germany

Summary

The size of a pool of readily releasable vesicles at a giant brainstem synapse, the calyx of Held, was probed with three independent approaches. Using simultaneous pre- and postsynaptic whole-cell recordings, two forms of presynaptic Ca^{2+} stimuli were applied in rapid succession: uncaging of Ca^{2+} by flash photolysis and the opening of voltage-gated Ca^{2+} channels. The ensuing transmitter release showed a nearly complete cross-inhibition between the two stimuli, indicating the depletion of a limited pool of about 700 transmitter quanta. The pool size was confirmed in experiments using enhanced extracellular Ca^{2+} concentrations, as well as short, high-frequency stimulus trains. The results reveal a surprisingly large pool of functionally available vesicles, of which a fraction of about 0.2 is released by a single presynaptic action potential under physiological conditions.

Introduction

Depletion of a pool of readily releasable transmitter quanta during trains of presynaptic action potentials has often been proposed as a mechanism for synaptic short-term depression (Elmquist and Quastel, 1965; Kusano and Landau, 1975; for reviews, see Zucker, 1996; Neher, 1998). However, depletion is difficult to prove directly, and alternative mechanisms, such as presynaptic Ca^{2+} current inactivation (Dobrunz et al., 1997; Forsythe et al., 1998), postsynaptic receptor desensitization (Trussell et al., 1993; Otis et al., 1996), or autoinhibition via presynaptic metabotropic receptors (Barnes-Davies and Forsythe, 1995; von Gersdorff et al., 1997) might participate in the generation of short-term depression. To define the role of vesicle pool depletion in short-term depression at a given synaptic connection, it is of crucial importance to know the size of a pool of readily releasable transmitter quanta (Rosenmund and Stevens, 1996), as well as the fraction of the pool that is released during a single presynaptic action potential. This "released fraction" (Reyes et al. 1998) will set the rate at which the pool is depleted during repetitive stimulation and is therefore a crucial parameter for determining the short-term plasticity behavior at a given synapse.

The axosomatic synapse of the calyx of Held, located in the superior olivary complex, is an attractive model system for studying synaptic depression, because the large calyceal terminal allows a direct investigation of presynaptic electrophysiological properties (Forsythe, 1994; Borst et al., 1995), and synaptic transmission undergoes a rapid, frequency-dependent depression upon repetitive stimulation (Borst et al., 1995; von Gersdorff et al., 1997; Wang and Kaczmarek, 1998). Nevertheless, the extent to which depletion of a pool of readily releasable quanta contributes to synaptic depression at the calyx of Held is not clear at present. This is because there are no estimates of the total pool of readily releasable quanta, nor of the fraction of the pool that is released during a single action potential (but see Chuhma and Ohmori, 1998).

We have addressed the question of pool size by employing three independent approaches, which all aimed at maximizing the Ca^{2+}-evoked transmitter output during short time intervals. Excitatory postsynaptic currents (EPSCs) mediated by AMPA-type glutamate receptors were recorded as a measure of presynaptic transmitter release. By combining this assay with presynaptic uncaging of Ca^{2+} by flash photolysis, we demonstrate a nearly complete cross-inhibition between transmitter release evoked by the opening of presynaptic, voltage-gated Ca^{2+} channels and the release evoked by rapid uncaging of presynaptic Ca^{2+}. The summed responses to paired stimuli at short time intervals were used to estimate the pool size. Moreover, the pool was probed by elevating extracellular Ca^{2+} concentration, as well as by short, high-frequency trains of stimuli. Taken together, the results show that there are about 700 transmitter quanta immediately available for release at the calyx of Held and that a single presynaptic action potential evokes the release of a fraction of about 0.2 of the total pool.

Results

Our first approach to estimate the number of immediately available transmitter quanta was an attempt to saturate transmitter output with high extracellular Ca^{2+} concentration ($[Ca^{2+}]_e$). If release probability under control conditions is close to maximal, as has been suggested recently for the calyx of Held (Chuhma and Ohmori, 1998), then elevating $[Ca^{2+}]_e$ should not increase the quantal content of EPSCs. If, however, only a submaximal fraction of the pool is released with each action potential, then it can be expected that a larger fraction of the readily releasable pool is recruited by increasing the presynaptic Ca^{2+} influx. Extrapolation to values of saturating $[Ca^{2+}]_e$ should give a lower limit for the estimate of the number of readily releasable transmitter quanta.

EPSCs were evoked by fiber stimulation at 0.1 Hz, a frequency at which the effect of cumulative depression on EPSC amplitude is negligible (von Gersdorff et al., 1997). When $[Ca^{2+}]_e$ was elevated from 2 mM to 4 mM and 10 mM, EPSC amplitudes were potentiated 2.23 ±

*To whom correspondence should be addressed (e-mail: rschneg@gwdg.de).

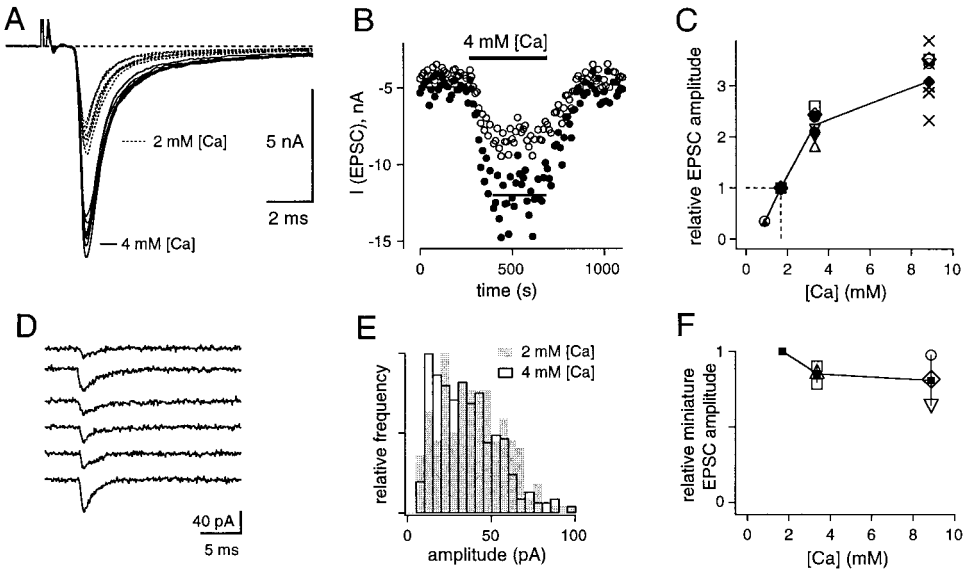

Figure 1. Release Probability at the Calyx of Held Synapse Is Not Maximal during Normal Synaptic Transmission

(A) Elevating $[Ca^{2+}]_e$ from 2 mM to 4 mM potentiates EPSC amplitudes measured in a MNTB principal cell after afferent fiber stimulation. Holding potential, −80 mV.

(B) Time plot of EPSC amplitudes from the same experiment as shown in (A). Open symbols represent measured peak amplitudes; closed symbols were obtained by correcting for the estimated voltage-clamp error (see Experimental Procedures).

(C) EPSC amplitudes, relative to the value at 2 mM $[Ca^{2+}]_e$, determined by 23 applications of different $[Ca^{2+}]_e$ in a total of n = 16 cells. Crosses represent data points obtained under partial block of postsynaptic AMPA receptors with 70 nM NBQX.

(D) Examples of spontaneously occurring miniature EPSCs at 2 mM $[Ca^{2+}]_e$.

(E) mEPSC amplitude distribution for the same cell as shown in (D), for 2 mM and 4 mM $[Ca^{2+}]_e$. The mean of the distribution was reduced from 39.4 pA at 2 mM $[Ca^{2+}]_e$ (n = 186 events) to 35.5 pA at 4 mM $[Ca^{2+}]_e$ (n = 362 events).

(F) mEPSC amplitudes estimated as in (E), relative to the value at 2 mM $[Ca^{2+}]_e$. There was a slight reduction of amplitudes at elevated $[Ca^{2+}]_e$. At 2 mM $[Ca^{2+}]_e$, an average mEPSC amplitude of 28.7 ± 8 pA (n = 9 cells) was found.

0.25–fold (n = 7) and 3.17 ± 0.48–fold (n = 7), respectively (Figures 1A, 1B, and 1C). To verify that this effect was caused by an increase in presynaptic release probability, we recorded spontaneously occurring miniature EPSCs (mEPSCs) in a different set of cells and quantified the effects of $[Ca^{2+}]_e$ on average mEPSCs amplitudes (Figures 1D, 1E, and 1F). The amplitude distributions revealed a slight shift toward smaller values (Figures 1E and 1F; n = 10 cells), compatible with a small blocking effect of extracellular Ca^{2+} on AMPA-type glutamate receptor channels (Jonas et al., 1993). These results indicate that the effects of $[Ca^{2+}]_e$ on evoked EPSC amplitudes resulted from an increase in quantal content. Voltage clamp errors (see Experimental Procedures) probably did not limit our measurement of EPSC amplitude potentiation, since the degree of potentiation with 10 mM $[Ca^{2+}]_e$ was similar (3.05 ± 0.46–fold, n = 8; see cross symbols in Figure 1C) when EPSCs were blocked to 33% ± 5% of the initial control amplitude with 70 nM NBQX, an antagonist of AMPA-type glutamate receptors.

When quantal content is analyzed as a function of $[Ca^{2+}]_e$, it is implicitly assumed that a linear relationship exists between extracellular Ca^{2+} concentration and the intracellular Ca^{2+} concentration that drives the vesicle fusion (Dodge and Rahamimoff, 1967; Reid et al., 1998). While this assumption might hold in the range of low $[Ca^{2+}]_e$, at higher concentrations the flux through voltage-gated Ca^{2+} channels is likely to saturate (see Church and Stanley, 1996, for the case of L-type Ca^{2+} channels). Since a saturation of Ca^{2+} influx would limit transmitter output at elevated $[Ca^{2+}]_e$, we measured Ca^{2+} influx with single action potentials, by combining presynaptic membrane potential recordings with Ca^{2+} imaging (Figure 2). Fura-2 (200 μM) was used in these experiments, a concentration that is sufficiently high to override the endogenous Ca^{2+}-buffering capacity of the presynaptic calyces (Helmchen et al., 1997). Therefore, the change in fluorescence at the Ca^{2+}-sensitive excitation wavelength (ΔF_{380} in Figure 2B) should be an accurate measure of the overall Ca^{2+} entering during an action potential (see Experimental Procedures).

Figure 2 shows an example for Ca^{2+} influx measurements when $[Ca^{2+}]_e$ was changed from 2 to 10 mM. As can be seen in Figure 2B, the 5-fold increase in $[Ca^{2+}]_e$ only led to a roughly 2-fold increase of the presynaptic Ca^{2+} influx. Similar experiments were done for the range of 1–10 mM $[Ca^{2+}]_e$, at a constant Mg^{2+} concentration of 1 mM (Figure 2D; n = 6 cells). This data set was fitted with a simple Michaelis-Menten saturation equation, which indicates a strong saturation of Ca^{2+} influx, with half-maximal values at roughly 2.6 mM $[Ca^{2+}]_e$. Additional experiments were done at 15 mM $[Ca^{2+}]_e$ with no added Mg^{2+}, in order to further increase the presynaptic Ca^{2+} influx (Figure 2D; Figure 3). At $[Ca^{2+}]_e$ of 10 mM or larger, we also observed changes in the presynaptic action potential waveform (Figure 2A; Table 1), compatible with the effects of extracellular Ca^{2+} ions on the gating of voltage-dependent ion channels (Frankenhaeuser, 1957).

The pronounced saturation of presynaptic Ca^{2+} influx

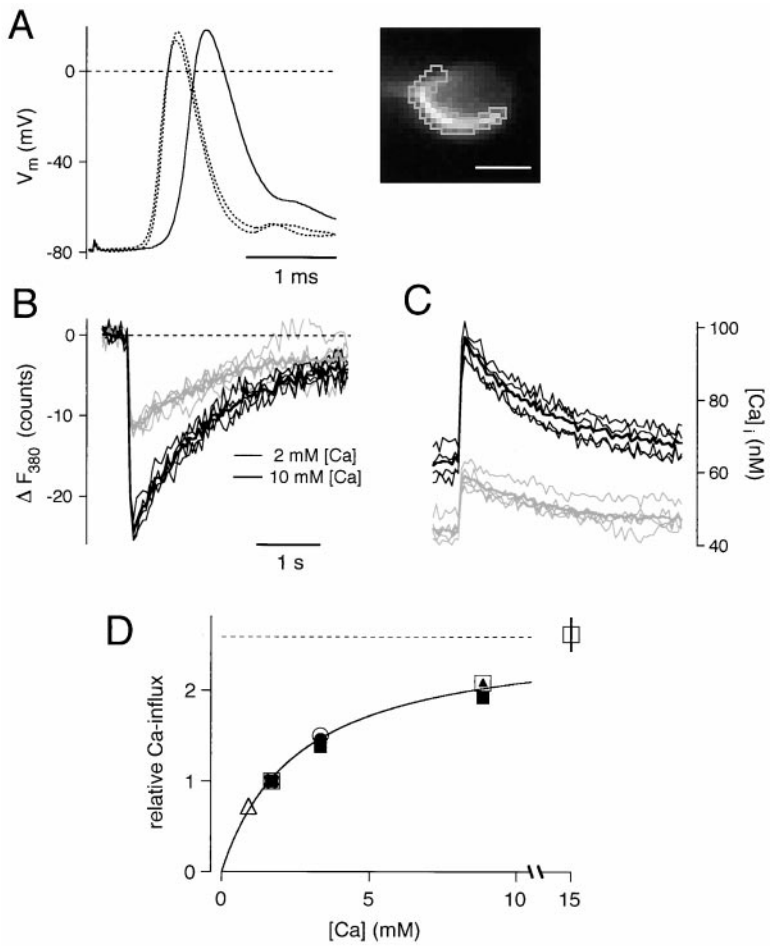

Figure 2. Saturation of Presynaptic Ca^{2+} Influx with Enhanced External Ca^{2+} Concentrations

(A) Single presynaptic action potentials evoked by afferent fiber stimulation at 2 mM $[Ca^{2+}]_e$ (dotted traces indicate control and recovery) and at 10 mM $[Ca^{2+}]_e$. Averages of five traces are shown. The inset shows the binned fluorescence image of the same calyx at 380 nm excitation, with the region of interest used to measure ΔF_{380} traces (see Experimental Procedures). Scale bar, 10 μm.

(B) Ca^{2+}-sensitive fluorescence change (ΔF_{380}) with single presynaptic action potentials at 2 mM and at 10 mM $[Ca^{2+}]_e$. Note that Ca^{2+} influx is roughly doubled for the change of $[Ca^{2+}]_e$ from 2 to 10 mM.

(C) Changes in intracellular free Ca^{2+} concentration, $[Ca^{2+}]_i$, for the same cell as shown in (A) and (B). Note the small increase in basal $[Ca^{2+}]_i$ when the extracellular Ca^{2+} concentration was 10 mM.

(D) Plot of Ca^{2+} influx relative to the value at 2 mM $[Ca^{2+}]_e$, determined as shown in (B) (n = 7 cells). The data were fitted with Equation 2, yielding an apparent half-maximal Ca^{2+} influx at 2.6 mM $[Ca^{2+}]_e$. The data point at 15 mM $[Ca^{2+}]_e$ was not included in the fit because of the different extracellular Mg^{2+} concentration.

is expected to limit the transmitter output at high $[Ca^{2+}]_e$. In order to account for this effect, relative EPSC amplitudes were plotted directly as a function of presynaptic Ca^{2+} influx (Figure 3). To ensure a strong potentiation of EPSC amplitudes, an additional series of experiments was done at 15 mM $[Ca^{2+}]_e$ with no added Mg^{2+}, a condition that induced a 4.08 $\pm$ 1.24–fold (n = 6 cells) potentiation of EPSC amplitudes. At 15 mM $[Ca^{2+}]_e$, the rising phase of EPSCs were not significantly changed with respect to the value at 2 mM $[Ca^{2+}]_e$ (Borst and Sakmann, 1996) (20%–80% rise times were 0.22 $\pm$ 0.04 ms and 0.24 $\pm$ 0.05 ms for 2 and 15 mM $[Ca^{2+}]_e$, respectively; see also Discussion). The plot of relative EPSC amplitudes versus Ca^{2+} influx in Figure 3 shows that the EPSC potentiation is gradually leveling off for Ca^{2+} influx values larger than the ones obtained at 2 mM $[Ca^{2+}]_e$. This behavior is more apparent when the fit of the data with the Hill equation (Figure 3, continuous line) is compared with a simple power function with the same cooperativity (Figure 3, broken line). The fit of the Hill equation predicts a saturation of transmitter output close to the observed maximal values, at an estimated quantal content of roughly 700 (Figure 3).

The analysis in Figure 3 indicates that the presynaptic Ca^{2+} sensors for transmitter release become saturated at increased Ca^{2+} influx. It is, however, not known whether release probability is close to unity at fully occupied Ca^{2+} sensors, because the short duration of the Ca^{2+} current during an action potential (Borst and Sakmann, 1996) might also limit the amount of vesicles that can undergo fusion (see also Discussion). If release probability at saturating Ca^{2+} influx was significantly smaller than unity, an underestimation of the pool size would result. It was therefore important to obtain independent estimates for the size of the readily releasable pool of transmitter quanta. We next applied an approach that made use of repetitive stimulation (n = 20 stimuli at 100 Hz), which induced a strong depression of EPSC amplitudes (Figure 4A; see also Borst et al., 1995; Wang and Kaczmarek, 1998). If it is assumed that depression is largely caused by a transient decrease in the number of readily releasable quanta, it should be possible to estimate the pool size by calculating the cumulative EPSC amplitudes for time intervals that are short with respect to the time required for recovery from depression (see von Gersdorff et al., 1997; Dittman and Regehr, 1998; Wang and Kaczmarek, 1998).

A series of such depression experiments was performed both at 2 mM and at 4 mM $[Ca^{2+}]_e$ to ensure conditions of elevated release probability (Figure 4). The change in $[Ca^{2+}]_e$ from 2 mM to 4 mM induced a 2.62 $\pm$ 0.47–fold potentiation of the amplitudes of the first EPSC

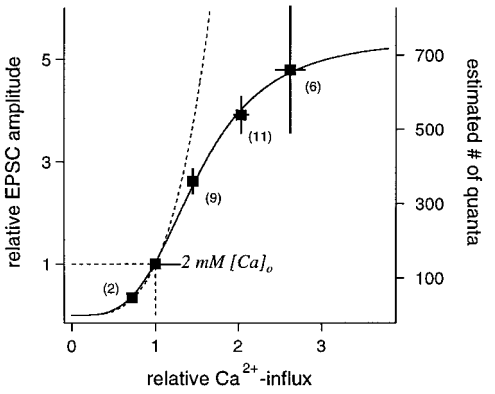

Figure 3. Extrapolation of Maximal Quantal Content for Saturating Values of Ca^{2+} Influx

Average values of relative EPSC amplitudes from Figure 1C were corrected for the (small) reduction of mEPSC amplitude (Figure 1F) and plotted directly as a function of relative Ca^{2+} influx, J_{Ca} (Figure 2D). Measurements were done at 1, 2, 4, and 10 mM $[Ca^{2+}]_e$ in the presence of 1 mM Mg^{2+}, and at 15 mM $[Ca^{2+}]_e$ with no added Mg^{2+} (see right-most data point). The quantal content on the right hand axis was estimated from the average EPSC amplitude at 2 mM $[Ca^{2+}]_e$, which was 3.92 ± 2.4 nA (n = 21 cells), corresponding to an estimated average quantal content of about 140. The data were fitted with the Hill equation (Equation 3; see continuous line). The fit parameters (Y_{max}/Y_{2Ca} = 5.4; K = 1.5, n = 3.5) indicate a maximal quantal content 5.4 times larger than that during average transmission at 2 mM $[Ca^{2+}]_e$, which corresponds to an estimated maximal value of 750 quanta. The dotted line is a power function ($Y = J_{Ca}^{3.5}$) to illustrate the saturating character of the Hill equation for Ca^{2+} influx values larger than the ones obtained at 2 mM $[Ca^{2+}]_e$.

(n = 5), confirming the data shown in Figure 1 for stimulation frequencies of 0.1 Hz. In four of five cells tested, the same increase in $[Ca^{2+}]_e$ also produced a shift from facilitation to depression, when the second EPSC amplitude was compared to the first one (see arrowheads in Figure 4A and filled symbols in Figure 4D). This finding is compatible with the interpretation that release probabilities are increased at elevated $[Ca^{2+}]_e$. EPSC amplitudes and cumulative EPSC amplitudes during 100 Hz trains were plotted versus time as shown in Figures 4B and 4C. To estimate cumulative EPSC amplitudes, a line was fitted to the steady state region for times larger than 100 ms and back-extrapolated to time 0 (Figure 4C). This estimate effectively takes into account the cumulative EPSC amplitudes reached within the first five to six stimuli, corresponding to a time interval of about 50 ms, before depression reaches its steady state level.

The average results of this approach are summarized in Figure 4E. Cumulative EPSC amplitudes at 4 mM $[Ca^{2+}]_e$ were slightly, but significantly, larger than the corresponding values at 2 mM $[Ca^{2+}]_e$ ($p < 0.02$, Student's t test). To test the validity of the assumption that recovery from depression is negligible for the time interval of about 50 ms used for this analysis, EPSC amplitudes were measured at 50 ms following the 200 ms trains at 100 Hz. It was found that EPSC amplitudes had recovered to 1.8% ± 0.6% and 4.4% ± 1.2% of their initial control amplitudes at 2 and 4 mM $[Ca^{2+}]_e$, respectively (n = 5 cells). Therefore, recovery from synaptic depression during the time interval used for calculating cumulative EPSC amplitudes should not have significantly influenced the pool size estimates obtained from the 100 Hz trains. Although the reasons for the difference in pool size estimate between the two extracellular Ca^{2+} concentrations are not fully understood at present, it is seen that the cumulative EPSC amplitudes at 4 mM $[Ca^{2+}]_e$ correspond to about 600 transmitter quanta, when the average mEPSC amplitude (28.7 ± 8 pA; n = 9 cells; see Figure 1) is considered. This value confirms the pool size estimate derived from the first approach (Figure 3).

The second pool size estimate relies on the assumption that Ca^{2+} influx with each action potential during a 100 Hz train stays equally effective in inducing transmitter release. Since this is not known for certain (see also Forsythe et al., 1998; Borst and Sakmann, 1999), it was necessary to obtain a third estimate using strong Ca^{2+} stimuli for neurotransmitter release. For this approach, we designed a "cross-depletion" experiment for two different types of Ca^{2+} stimuli: the physiological Ca^{2+} stimulus produced by the opening of voltage-gated Ca^{2+} channels and an artificial Ca^{2+} stimulus produced by flash photolysis of the caged Ca^{2+} compound, DM-nitrophen (Kaplan and Ellis-Davies, 1988; Delaney and Zucker, 1990). If either of the two stimuli induces the release of a large fraction of the readily releasable pool of transmitter quanta, a marked cross-inhibition of transmitter release should result.

Paired recordings of presynaptic calyces and postsynaptic principal cells were made at 2 mM $[Ca^{2+}]_e$, with a presynaptic pipette solution containing 1 mM DM-nitrophen, loaded with approximately 0.85 mM Ca^{2+} (see Experimental Procedures). After allowing for equilibration of the pipette solution with the presynaptic cytosol (about 4 min), a short (1.5 ms) light flash at maximal intensity of the flash lamp was given to photolyze DM-nitrophen. This induced a rapid increase in intracellular free Ca^{2+} concentration, which was measured with the low-affinity Ca^{2+} indicator, fura-2 FF (Figures 5A and 5B). The postsynaptic cell responded with a rapidly rising and decaying (τ_{decay} = 3.4 ± 1.5 ms, n = 12), large current (9.23 ± 5.1 nA, n = 14; see Figures 5Cb, 5E, and 6). The fast kinetics of these responses, as well as the modulation of their decay times by cyclothiazide (see

Table 1. Parameters of Presynaptic Action Potential Waveforms at Two External Ca^{2+} Concentrations

External Ca^{2+} Concentration	Latency (ms)	Rate of Rise (mV/ms)	Half Width (ms)	Amplitude (mV)
2 mM $[Ca^{2+}]_e$	0.71 ± 0.05	526 ± 67	0.55 ± 0.13	104.1 ± 6.3
10 mM $[Ca^{2+}]_e$	0.90 ± 0.07[a]	361 ± 91[b]	0.74 ± 0.14[b]	103.7 ± 8.6

Average values from pairwise comparison in n = 3 cells are given. Symbols indicate significant differences at the $p < 0.01$ ([a]) and $p < 0.05$([b]) level, respectively, according to paired Student's t test.

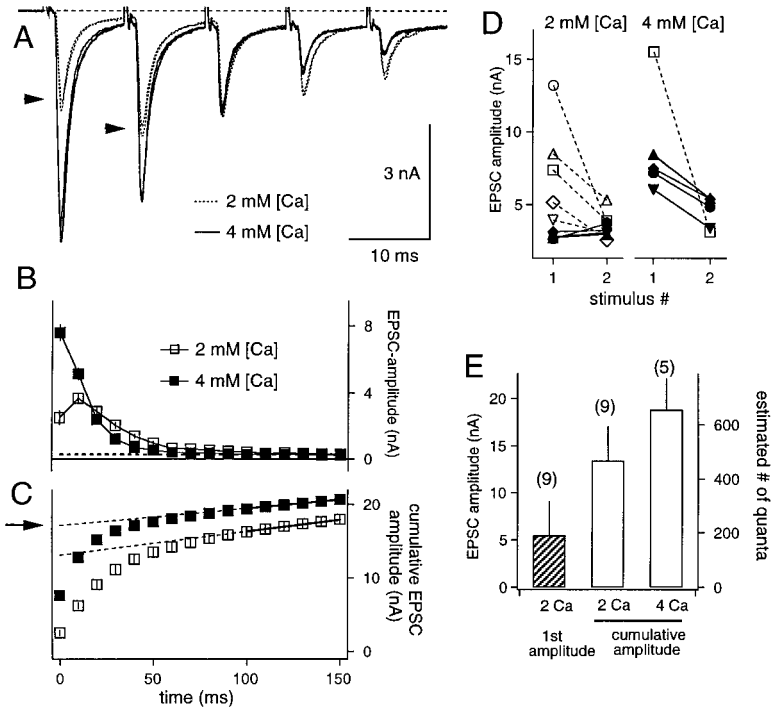

Figure 4. Cumulative EPSC Amplitudes with 100 Hz Stimulation Confirms the Pool Size Estimate

(A) Responses to the first five stimuli of 100 Hz trains for one cell, in the presence of either 2 mM or 4 mM $[Ca^{2+}]_e$. Note that the paired-pulse ratio between the first two pulses was inverted by changing $[Ca^{2+}]_e$ from 2 mM to 4 mM (arrowheads). A similar behavior was observed in four out of five cells, as shown in (D) (filled symbols).

(B) Analysis of peak EPSC amplitudes for the cell shown in (A). Average for five trains each are shown.

(C) Peak EPSC amplitude values were integrated to give a plot of cumulative EPSC amplitudes during 100 Hz trains. Data points in a range of 100–200 ms were fitted by linear regression, and back-extrapolated (dotted line) to time 0, to estimate the cumulative EPSC amplitudes before steady state depression.

(D) EPSC amplitude values for the first and second stimulus during 100 Hz trains, both at 2 mM $[Ca^{2+}]_e$ (left panel; n = 9 cells) and at 4 mM $[Ca^{2+}]_e$ (right panel; n = 5 cells).

(E) Summary of EPSC amplitudes, and cumulative EPSC amplitudes analyzed as shown in (C). Left bar, average EPSC amplitude for the first stimulus at 2 mM $[Ca^{2+}]_e$. Middle bar, average cumulative EPSC amplitude at 2 mM $[Ca^{2+}]_e$, determined as shown in (C). Right bar, average cumulative EPSC amplitude at 4 mM $[Ca^{2+}]_e$. The number of cells is indicated in brackets.

below; Figure 6), indicated that they were mediated by AMPA-type glutamate receptors.

Double pulses of presynaptic membrane depolarizations (1.5 ms to +28 mV, V_h −80 mV) evoked large Ca^{2+} currents, with average charge transfer of 3.82 ± 0.98 pC and 3.87 ± 0.95 pC for the first and second current, respectively (Figure 5C, thin trace). This value is about four times larger than the Ca^{2+} charge entering with a single action potential at 2 mM $[Ca^{2+}]_e$ (0.8–1.0 pC; Borst and Sakmann, 1996; Helmchen et al., 1997) and should therefore represent a strong stimulus for transmitter release. The postsynaptic cell responded to these Ca^{2+} currents with two successive EPSCs with decreasing peak amplitude (Figures 5Ca, 5E, and 6).

Transmitter release induced by flash photolysis and by presynaptic double depolarizations showed a strong cross-inhibition, as is illustrated in Figure 5C for one representative experiment. Control responses to presynaptic double depolarizations were established first (Figure 5Ca). In Figure 5Cb, the double depolarization was preceded by a maximal flash, the response of which strongly depressed the EPSCs evoked by the presynaptic Ca^{2+} currents. This depression was reversible, since a control double-pulse depolarization given 64 s later evoked a response similar to the one shown in Figure 5Ca (data not shown). Moreover, the depression was not accompanied by a significant change in the Ca^{2+} charge evoked by the depolarizations (3.82 ± 0.98 pC in control versus 3.63 ± 0.78 pC after flashes, n = 7 cells). At a later time in the same experiment (Figure 5Cc), the sequence of flash and double depolarization was inverted. The double depolarization evoked a similar EPSC to the one obtained under control conditions, but the flash-evoked response was now largely depressed. Thus, there was a marked cross-inhibition of transmitter release evoked by the two different Ca^{2+} stimuli, which is summarized in Figure 5D.

We hypothesize that cross-inhibition of EPSCs is a consequence of the limited size of a pool of immediately available transmitter quanta, which is largely depleted by each of the two types of Ca^{2+} stimuli. In this case, cross-inhibition should be use dependent. To test this prediction, a series of experiments was performed in which flashes of variable intensities were followed by double depolarizations (Figure 5E). Flashes that were attenuated to 10% or 20% by the use of neutral density filters induced small EPSCs with slow rise times. Such EPSCs only caused a small degree of inhibition of the subsequent, depolarization-evoked EPSCs and, in some cases, even led to a facilitation of the subsequent responses (data not shown; Kamiya and Zucker, 1994). The unattenuated flash, on the other hand (Figure 5E), evoked a rapidly rising, large, and fast EPSC, which induced a full inhibition of the subsequent EPSC. These observations, which were made in a total of n = 4 cells, show that inhibition of EPSCs by a preceding flash-evoked EPSC is use dependent, compatible with the idea of pool depletion.

To address the possibility that cross-inhibition occurred through a mechanism involving postsynaptic receptor desensitization, we performed control experiments with cyclothiazide (CTZ), which should inhibit

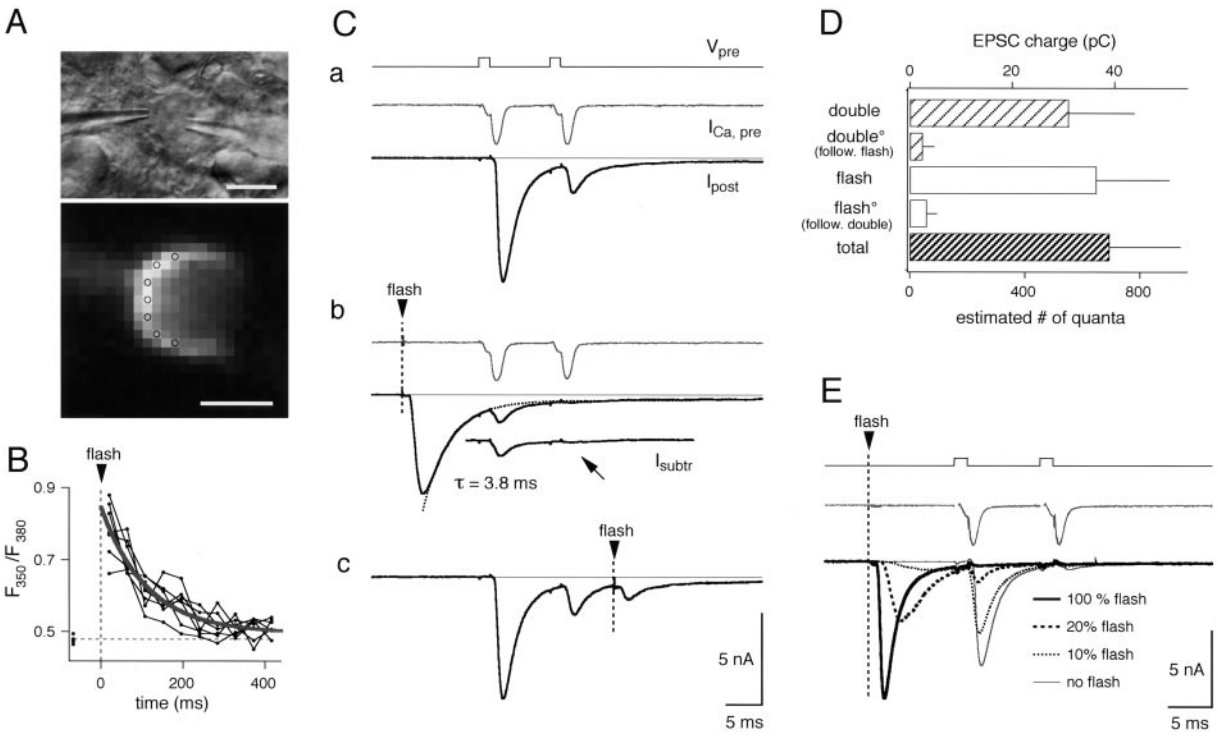

Figure 5. Cross-Inhibition of Transmitter Release by Two Independent Ca^{2+} Stimuli Indicates Depletion of a Pool of Immediately Available Transmitter Quanta

(A) Transmission image (upper panel) and fluorescence image (lower panel) during simultaneous pre- and postsynaptic whole-cell recording. The presynaptic patch-pipette solution contained 1 mM Ca^{2+}-loaded DM-nitrophen and 0.1 mM of the low-affinity Ca^{2+} indicator, fura-2 FF (see Experimental Procedures).

(B) A short (about 1.5 ms) flash of UV light caused a rapid increase in the fura-2 FF fluorescence ratio measured from the pixels indicated in (A). The decay of the fluorescence ratio was fitted with an exponential function (τ = 112 ms), which was back-extrapolated to the time of the flash (vertical dotted line).

(C) Cross-depletion experiment.

(Ca) Presynaptic Ca^{2+} currents ($I_{Ca, pre}$) and EPSCs (I_{post}) induced by a double depolarization (V_{pre}) from −80 mV to +28 mV, 1.5 ms duration. Ca^{2+} current was leak-subtracted with a P/4 protocol.

(Cb) Same double pulse, but preceded by 10 ms by a maximal flash. The decay of the flash-evoked EPSC was fitted with an exponential function (τ = 3.8 ms), which was extrapolated to longer times (dotted line) and then used to generate the subtraction current (I_{subtr}).

(Cc) Response to a maximal flash given 10 ms after a double-pulse depolarization. The response to the double depolarization is restored to control (see Ca), whereas the flash-evoked EPSC is now largely depressed.

(D) Average EPSC charge induced by double pulses of presynaptic depolarizations (double, n = 12), double pulses following maximal flashes (double°, n = 12), maximal flashes (flash, n = 12), flashes following the double pulses (flash°, n = 3), and the total charge transfer of the sequences flash followed by double pulse (total, n = 12). The number of quanta was estimated by dividing the charge values by the average charge transfer of mEPSCs.

(E) The inhibition by the flash-evoked EPSCs is use dependent. Flashes were attenuated to the indicated values by using neutral density filters. Weak flashes, which evoked smaller and more slowly rising EPSCs, also caused a smaller degree of inhibition of the subsequent depolarization-evoked EPSCs.

(Trussell et al., 1993; Yamada and Tang, 1993), or at least largely slow down (Partin et al., 1994), the desensitization of AMPA receptors, depending on the exact pattern of AMPA receptor splice variants expressed in MNTB principal cells (Geiger et al., 1995; Caicedo and Eybalin, 1999). The response of the synapses to double-pulse depolarizations (Figure 6A, gray trace) and the inhibition of this response by a preceding flash was first tested in control external solutions (Figure 6A). The external solution was then switched to 100 μM CTZ, and double depolarizations were given until the effects of CTZ had stabilized (see gray trace in Figure 6B). Subsequently, another flash, followed by a double depolarization, was applied to test for inhibition of transmitter release (Figure 6B, thick trace).

To analyze the effects of CTZ, the ratio between the EPSC evoked by the first depolarization following the flash (labeled I_1 in Figure 6) and the flash-evoked EPSC itself (I_{flash} in Figure 6) was quantified. This ratio was 0.098 ± 0.057 in control versus 0.153 ± 0.073 in the presence of CTZ (mean ± SEM, respectively, n = 6); indicating that the inhibition of depolarization-evoked EPSCs by previous flash responses was not significantly different in the presence of CTZ. We interpret this finding to indicate that desensitization is not the main cause for the cross-inhibition of EPSCs induced by the two Ca^{2+} stimuli. CTZ also prolonged the decay time of EPSCs evoked by flashes and by depolarizations (compare Figures 6A and 6B), and it induced an increase of the flash-evoked EPSC amplitudes to 147% ± 31% of

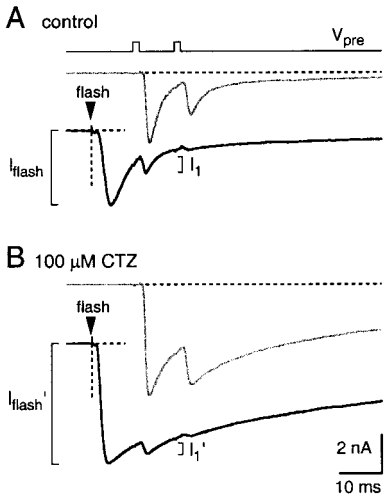

Figure 6. Inhibition of EPSCs by Preceding Flash-Evoked Transmitter Release Is Not Suppressed by Cyclothiazide (CTZ), an Inhibitor of AMPA Receptor Desensitization

(A) Responses to double depolarizations (gray trace) and to the sequence maximal flash-double depolarization (black trace) in control external solutions. Note the strong depression of the depolarization-evoked EPSCs, which is manifest in a small ratio of I_1/I_{flash}.

(B) Same cell, after complete wash-in of 100 μM CTZ into the extracellular solution. Note that the ratio I_1/I_{flash} was nearly unchanged with respect to control.

control (n = 6; see Figure 6). It is likely that this latter effect results from the fact that transmitter release after flash photolysis occurred slightly asynchronously, in a time window of about 1–5 ms. Since CTZ prolonged the time course of mEPSCs at the calyx of Held (T. Sakaba and E. N., unpublished data; see also Yamada and Tang, 1993, and Diamond and Jahr, 1995, for the case of hippocampal neurons), it is expected that larger peak EPSC amplitudes are obtained in the presence of CTZ, because prolonged mEPSC waveforms should add up to larger peak EPSCs when release occurs asynchronously. However, an additional small presynaptic effect of CTZ (Barnes-Davies and Forsythe, 1995; Diamond and Jahr, 1995) cannot be excluded at present. Nevertheless, such an effect should not invalidate our conclusion that cross-inhibition of transmitter release (Figures 5 and 6) is largely mediated by a depletion of a pool of readily releasable transmitter quanta.

Since the combination of a maximal flash and the first depolarization largely depleted the pool of available quanta (note the absence of responses to the second depolarizations; Figures 5Cb and 6B), the summed postsynaptic charge transfer after the combination of the two stimuli should reflect the size of the readily releasable pool. Charge transfer was analyzed, because the rise and decay times of the flash-evoked responses indicate that release occurred slightly asynchronously, which would lead to an underestimation of quantal content if peak amplitudes were analyzed. In the absence of CTZ, the total charge transfer with the sequence of flash followed by double depolarization was found to be 39.1 ± 13.9 pC (Figure 5D; n = 12 cells; range, 22–69 pC). This value, divided by the average quantal charge at 2 mM $[Ca^{2+}]_e$ (see Experimental Procedures), gave an average pool size estimate of 695 transmitter quanta (range, 390–1220 quanta).

Discussion

We have estimated the number of readily releasable transmitter quanta at a large, auditory brainstem synapse, the calyx of Held, by using three independent approaches, which gave converging results. In the first approach, we have attempted to maximize the transmitter output during EPSCs, by elevating the extracellular Ca^{2+} concentration ($[Ca^{2+}]_e$), and the quantal content for saturating presynaptic Ca^{2+} influx was extrapolated (Figure 3). In a second approach, repetitive fiber stimulation at high frequencies was used to depress synaptic transmission, and cumulative EPSC amplitudes were calculated for short time intervals (Figure 4). In a third approach, two independent, strong Ca^{2+} stimuli for transmitter release were given in close temporal succession, which induced a marked cross-inhibition of transmitter release, a finding that allowed us to use the summed responses for a pool size estimate (Figure 5). The resulting values indicate that there are about 700 transmitter quanta available for immediate release, of which roughly one fifth, or in some cells more (Figure 4D), is released by single action potentials under conditions of normal release probability at 2 mM $[Ca^{2+}]_e$.

Saturation of Transmitter Release with Increased Presynaptic Ca^{2+} Influx

Transmitter output during EPSCs evoked by afferent fiber stimulation was not maximal at 2 mM $[Ca^{2+}]_e$ (Figures 1 and 3). This result was surprising in the light of a previous paper that analyzed the postnatal development of transmission at the calyx of Held synapse of rats (Chuhma and Ohmori, 1998). Figure 6 of Chuhma and Ohmori (1998) suggested that EPSC amplitudes at a similar age as the one used here were not increased when $[Ca^{2+}]_e$ was changed from 2 to 5 mM. Also, by analyzing EPSC amplitude fluctuations, the release probability was estimated to be 0.87 at the calyx of Held of 9- to 11-day-old rats (Chuhma and Ohmori, 1998). Our finding, however, that EPSCs can be further potentiated up to 5-fold (Figure 3) shows directly that the fraction of the total pool that is released with a single action potential cannot be larger than about one-fifth for the average of the cells analyzed here. It seems difficult to decide at present whether the discrepancy between our estimate and the previous one (Chuhma and Ohmori, 1998) is due to technical differences or due to a different definition of release probability.

Ca^{2+} influx with single presynaptic action potentials showed a pronounced saturation, with a value of only 2.6 mM $[Ca^{2+}]_e$ for half-maximal Ca^{2+} influx (Figure 2). This effect, which probably results from a saturation of single channel conductance in Ca^{2+} channels (see Church and Stanley, 1996), has to be taken into account when a quantitative relationship between Ca^{2+} concentration and quantal content is derived. To do so, we plotted quantal content directly as a function of the presynaptic Ca^{2+} influx (Figure 3). This approach revealed that the relationship between quantal content and Ca^{2+} influx for the range of 2 to 10 mM $[Ca^{2+}]_e$ is

steeper than expected from the classical plot (Dodge and Rahamimoff, 1967), which uses extracellular Ca^{2+} concentrations (compare Figures 3 and 1C). Also, the plot of Figure 3 gives a basis for a fit of the Hill equation, which predicts a value of cooperativity in the range of 3 to 4, in good agreement with the range of cooperativity estimates at this (Borst and Sakmann, 1996; Wu et al., 1999) and other synapses (Dodge and Rahamimoff, 1967; Augustine et al., 1985; Heidelberger et al., 1994; Reid et al., 1998).

The fit of the Hill equation to the data in Figure 3 predicts a saturation of transmitter output at an estimated quantal content of about 700, a value that is congruent with the pool size estimates from two additional approaches (Figures 4–6 and Discussion below). An interpretation of this finding in terms of a kinetic scheme that assumes a series of Ca^{2+}-binding steps, followed by a final fusion reaction (Thomas et al., 1993; Heinemann et al., 1994) allows us to make some inferences about the limiting factors for transmitter release during single presynaptic action potentials at the calyx of Held. The finding that the rise times of EPSCs at 15 mM $[Ca^{2+}]_e$ were unchanged with respect to control (see Results) shows that the release process has a similarly short duration for the two conditions of Ca^{2+} influx. Since at high extracellular Ca^{2+} concentration ($[Ca^{2+}]_e \geq 10$ mM; see Figure 3), a large fraction of the pool can be released by a single action potential, it seems that neither the short duration of the Ca^{2+} influx signal (Borst and Sakmann, 1996) nor the rate constant of the final fusion reaction impose a limit on the amount of transmitter release. Under conditions of normal extracellular $[Ca^{2+}]$, the reduced transmitter release is therefore likely to be due to incomplete occupation of the Ca^{2+} sensors. The finding that transmitter output is not saturated at normal Ca^{2+} influx makes synaptic strength sensitive to a modest downregulation of presynaptic Ca^{2+} currents, which occurs after activation of metabotropic glutamate and $GABA_B$ receptors (Takahashi et al., 1996, 1998; Isaacson, 1998).

Depletion of a Pool of Synaptic Vesicles by Presynaptic Uncaging of Ca^{2+}

The use of the photolyzable Ca^{2+} chelator, DM-nitrophen, combined with simultaneous pre- and postsynaptic recordings, has allowed us to design a cross-depletion experiment (see also Heidelberger, 1998), in which two independent, strong Ca^{2+} stimuli were applied in rapid succession: uncaging of presynaptic cytosolic Ca^{2+} by flash photolysis and the opening of voltage-gated Ca^{2+} channels (Figure 5). Transmitter release evoked by presynaptic uncaging of Ca^{2+} inhibited the release evoked by subsequent depolarizing pulses in a use-dependent way (Figure 5E). Since this inhibition was not changed by cyclothiazide (Figure 6), an inhibitor of AMPA receptor desensitization, we hypothesize that cross-inhibition reflects the depletion of a limited pool of about 700 transmitter quanta.

If other mechanisms beside pool depletion contributed to the use-dependent inhibition of transmitter release, then an underestimation of the pool size would result from the analysis in Figure 5. In hippocampal neurons, one form of rapid synaptic depression was attributed to the inactivation of presynaptic Ca^{2+} channels and was found to be independent of previous transmitter release (Dobrunz et al., 1997); this form of depression was probably absent in our experiments because cross-inhibition was clearly use dependent (Figure 5E), and Ca^{2+} currents did not show inactivation under the conditions of the experiments shown in Figure 5. Similarly, adaptation of Ca^{2+}-triggered exocytosis (Hsu et al., 1996) probably did not contribute to cross-inhibition, because in that case, the use dependency of cross-inhibition (Figure 5E) could only be explained by postulating that exocytosis and adaptation have the same Ca^{2+} sensitivity. This, however, would make it difficult to distinguish between the effects of vesicle depletion and those of Ca^{2+} adaptation.

Another form of rapid depression in hippocampal synapses was found to be use dependent and recovered with a fast time constant of about 6 ms (Dobrunz et al., 1997). Its mechanism was referred to as "lateral inhibition" between vesicles in the release-ready pool (Dobrunz et al., 1997). Its fast time constant of recovery, however, makes this mechanism an unlikely candidate for depression at the calyx of Held. Depression induced by 100 Hz trains (Figure 4) had only recovered to 4.4% at a time interval of 50 ms (see Results), and complete recovery required intervals of several seconds (data not shown; see also von Gersdorff et al., 1997; Wang and Kaczmarek, 1998), compatible with the idea that a rather slow process determines the refilling of the readily releasable pool of vesicles (see Stevens and Wesseling, 1998, and references therein). Nevertheless, we cannot rule out at present that a mechanism of lateral inhibition is functional at the calyx of Held synapse. Also, it is difficult to rule out that with a strong enough Ca^{2+} stimulus, a resource other than vesicles in the readily releasable pool becomes limiting. The possibility exists that under CTZ, when EPSCs are extremely large, postsynaptic receptors might saturate. In that case, it is likely that the upper limit of pool size, presently estimated to be about 1200, might become even larger.

By showing a marked cross-inhibition between transmitter release evoked by uncaging of Ca^{2+} and by the opening of voltage-gated Ca^{2+} channels (Figures 5 and 6), we have isolated a strong form of synaptic depression that is located clearly downstream to presynaptic Ca^{2+} signaling. The summed responses to the two types of Ca^{2+} stimuli are in good agreement with the pool size estimates from two other experimental approaches (Figures 3 and 4). It seems, therefore, that the common mechanism that limits the transmitter output in the three types of experiments presented here is the finite number of transmitter quanta available for immediate release. If this conclusion is correct, it follows that the rapid phase of depression at the calyx of Held, which is complete within the first five to six stimuli of a high-frequency train (see Figure 4; Wang and Kaczmarek, 1998), is readily explained by a decrease of the number of immediately available transmitter quanta.

The Released Fraction and Total Pool at the Calyx of Held Synapse

Having established the total number of quanta that are immediately available for release (about 700 on average; range, 390–1220), we can estimate which fraction of

the pool is released during an action potential under conditions of normal release probability, that is, at 2 mM $[Ca^{2+}]_e$. In this definition, the released fraction (Reyes et al., 1998) equals the quantal content during an EPSC, divided by the pool size. This quantity should be equal to the average release probability for all the vesicles in the readily releasable pool. The average EPSC amplitude at 2 mM $[Ca^{2+}]_e$ for the analysis presented in Figure 3 was 3.9 ± 2.4 nA (range, 1.1–10.3 nA; n = 21 cells), indicating that the mean quantal content was roughly 140. This corresponds to a released fraction of about 0.2, when the pool size estimate of Figure 3 is considered.

This value should be regarded as an average estimate, because there is probably a cell-to-cell variability in both the total size of the pool, as well as in the released fraction. For example, in the data set used for Figure 4, a group of cells with small initial EPSC amplitudes (around 3 nA) and facilitating second responses was observed at 2 mM $[Ca^{2+}]_e$ (Figure 4D, closed symbols), whereas other cells had larger EPSCs with depressing second EPSCs even at 2 mM $[Ca^{2+}]_e$ (Figure 4D, open symbols). This might indicate a heterogeneity of average release probability between cells, in the sense that some cells might have higher average release probability of up to 0.5. This assumption would explain the increased depression of the second EPSC amplitudes in this group of cells (Figure 4D), as well as the finding that the initial rate of depression during 10 Hz trains is larger for cells with large initial EPSC amplitudes (S. Weis et al., submitted).

There was also a scatter in the pool size estimate (range, 390–1220 quanta; see Results) derived from the caged Ca^{2+} experiments. This might be caused by individual differences between presynaptic fibers, maybe as a function of their firing activity (Ryugo et al., 1996). Also, in the age range studied here (postnatal 8- to 10-day-old animals; see also Chuhma and Ohmori, 1998), pool size might depend on the developmental stage of the cell under study.

Possible Structural Correlate of the Pool of Immediately Available Quanta

It is interesting to speculate about the possible structural correlates of the pool of immediately available quanta, which we have identified here for the calyx of Held synapse. It seems safe to conclude from the present data that there are, on average, at least 700 docked vesicles, which can immediately undergo fusion upon a presynaptic Ca^{2+} signal. This number might represent a subset, or otherwise a fairly large fraction of the total pool of docked vesicles.

At many synapses, an analysis of amplitude fluctuations of synaptic currents indicates that the stochastic nature of transmitter release can be described by binomial statistics, and the binomial parameter "N" is often suggested to correspond to the total number of morphologically defined active zones (Zucker, 1973; Korn et al., 1981; Silver et al., 1998). In the case of calyceal synapses, ultrastructural features have been studied with electron microscopy (Lenn and Reese, 1966; Ryugo et al., 1996, and references therein); however, the total number of active zones has not yet been counted from reconstructions of complete calyces. For two calyceal terminals of the "end bulb of Held" type, located in the anteroventral cochlear nucleus of juvenile cats, the number of active zones has been more indirectly estimated to be around 400, or more than 1000, depending on the presynaptic fiber type (Ryugo et al., 1996). These values are of similar order of magnitude as our functional pool size estimate. Nevertheless, an answer to the question of whether the number of readily releasable quanta, for the developmental stage studied here, corresponds to the number of active zones must await a detailed morphological analysis.

Experimental Procedures

Electrophysiology and Slice Preparation

Transverse brainstem slices of 200 μm thickness were prepared with a vibratome, using postnatal 8- to 10-day-old rats, which were killed by decapitation according to institutional guidelines. Whole-cell patch-clamp recordings were made from visually identified postsynaptic principal cells of the medial nucleus of the trapezoid body (MNTB), in an experimental set-up with an upright microscope (Zeiss, Jena, Germany) and infrared gradient contrast illumination (Luigs and Neumann, Ratingen, Germany). Afferent presynaptic axons were stimulated with a bipolar electrode placed at about 300 μm from the recording site. Experiments were done at 21°C–24°C with extracellular solution containing (in mM) 125 NaCl, 25 $NaHCO_3$, 2.5 KCl, 1.25 NaH_2PO_4, 25 glucose, 1 $MgCl_2$, 0.4 ascorbic acid, 3 myo-inositol, and 2 Na-pyruvate (pH 7.4 when bubbled with 95% O_2, 5% CO_2). $CaCl_2$ was added at nominal concentrations ($[Ca^{2+}]_e$) of 1, 2, 4, or 10 mM. The corresponding free extracellular Ca^{2+} concentrations, which were lower because of Ca^{2+} binding to HCO_3^- (Martell and Smith, 1974) were estimated to be 0.91, 1.69, 3.35, and 8.86 mM by using a Ca^{2+}-sensitive electrode. For the plots in Figures 1C, 1F, and 2D, this correction was taken into account. An additional series of experiments (Figures 2D and 3) was done at 15 mM $[Ca^{2+}]_e$ with a solution containing (in mM) 150 NaCl, 10 HEPES, 2.5 KCl, 10 glucose, and 15 $CaCl_2$ (pH 7.4).

The internal solution contained (in mM) 130 K-gluconate, 20 KCl, 10 HEPES, 4 Mg-ATP, 0.3 GTP, and 5 EGTA (pH 7.2). EPSCs were recorded under whole-cell voltage-clamp at a holding potential of −80 mV, using an EPC9/2 patch-clamp amplifier (HEKA-Elektronik, Lambrecht, Germany). Series resistance (R_s; range, 4–8 MΩ at the beginning of the recording) was partially compensated and checked at regular intervals, such that a fixed value of 3 MΩ remained uncompensated. With this procedure, measured EPSC amplitudes at different times can be directly compared (Figure 1B, open symbols). The remaining deviation from holding potential (ΔV_h) was calculated off-line ($\Delta V_h = R_s \times I_{EPSC}$), and EPSC amplitudes were corrected (Figure 1B, closed symbols), assuming a reversal potential of 0 mV. The value of ΔV_h depended on the EPSC amplitude but did not exceed 25 mV for the data set.

Spontaneously occurring, miniature EPSCs were recorded with 10 μM bicuculline, 2 μM strychnine, and 0.5 μM TTX added to the external solution and were detected off-line by using a first-derivative threshold routine kindly provided by Dr. C. Pouzat. Results are presented as mean ± SD unless noted otherwise.

Measurements of Presynaptic Ca^{2+} Influx

The Ca^{2+}-imaging system (TILL photonics, Planegg, Germany) incorporated an interline transfer CCD chip and a monochromator providing excitation light at 357 and 380 nm wavelengths, which was dimmed to 10% with a neutral density filter. Background-corrected fluorescence-intensity traces at 380 nm excitation (ΔF_{380}) were constructed for regions of interest (see inset of Figure 2A), using series of 8 × 8 binned images taken with 20 ms exposure times at intervals of 50 ms. The Ca^{2+}-independent fluorescence at 357 nm wavelength was measured immediately before the stimulus, and the intracellular free Ca^{2+} concentration (Figure 2B) was calculated from the background-corrected fluorescence ratio according to the equation given by Grynkiewicz et al. (1985). The internal solution was the same as given above, except that EGTA was replaced by 200 μM

fura-2, a concentration sufficiently high to outcompete the endogenous Ca^{2+} buffer capacity of the calyx of Held terminals (Helmchen et al., 1997). Under this condition, changes in ΔF_{380} will reflect total Ca^{2+} influx (Neher, 1995).

Flash Photolysis Uncaging of Presynaptic Ca^{2+}

Ninety percent of the light output of a Xenon arc flash lamp (Rapp Optoelektronik, Hamburg, Germany) and 10% of the light output of the monochromator were combined into the epifluorescence port of the upright microscope, which was equipped with a 60×, 0.9 NA water-immersion objective (Olympus, Tokyo, Japan). The low-affinity Ca^{2+} indicator, fura-2 FF (TEFLABS, Texas) was excited alternately at 350 and 380 nm wavelengths, and fluorescence images at 8 × 8 pixel binning were taken with 20 ms exposure times. The fluorescence ratios of single pixels from the brightest regions of the calyx (Figure 5A) were analyzed following background subtraction.

The external solution was complemented with 0.5 μM TTX and 10 μM TEA. 7-chloro-kynurenic acid (30 μM) was added to assure a complete block of postsynaptic NMDA receptors (Kemp et al., 1988). At this concentration, 7-chloro-kynurenic acid also blocked AMPA receptor–mediated EPSCs to an estimated 75% of their control amplitude (n = 3 cells). Presynaptic pipette solutions contained 130 mM Cs-gluconate, 20 mM TEA, 20 mM HEPES, 1 mM DM-nitrophen (CalBiochem, Bad Soden, Germany), 0.85 mM $CaCl_2$, 0.5 mM $MgCl_2$, 5 mM Na_2-ATP, and 0.1 mM fura-2FF. We estimate that at equilibrium, 0.8 mM Ca^{2+} and 0.1 mM Mg^{2+} will be bound to DM-nitrophen (see also Heidelberger, 1998). Fura-2FF was calibrated in vitro using thin glass capillaries (VitroCom, Rockaway, NJ) giving limiting ratios (F_{350}/F_{380}) of 0.5 (at nominally Ca^{2+}-free fura-2 FF) and 6.5 (at saturating Ca^{2+}), and K_D of 10 μM of the fura-2 FF/Ca^{2+} complex, estimated by using intermediate Ca^{2+} concentrations (2.6, 8.4, and 28 μM) set by an appropriate mixture of $CaCl_2$ and DPTA, a Ca^{2+} buffer with low affinity (K_D = 80 μM). Maximal flashes raised presynaptic F_{350}/F_{380} ratios from 0.52 ± 0.04 to 0.91 ± 0.09 (n = 10 cells; see Figure 5B for an example). Considering the calibration constants, we estimate that roughly 50% of fura-2FF was bound to Ca^{2+} shortly after the flash. We have not yet attempted to estimate the free Ca^{2+} concentration at the time when transmitter release occurs (about 1–5 ms following the flash). An estimate at such short times would have to take into account the kinetic constants of the Ca^{2+}-binding substances (Xu et al., 1997), which, in the case of the endogenous Ca^{2+} buffers of calyces of Held, are not known.

Before integration of flash-evoked EPSCs, current traces were corrected point-by-point for the estimated voltage-clamp error. This correction led to an increase of about 20% in the total charge estimate. The contribution of a slow current component with amplitude of 0.14 ± 0.05 nA (n = 12) was subtracted to avoid an overestimation for the longest integration times (30 ms) with respect to the shorter ones (10 and 20 ms). The charge transfer for intervals of 30 ms after stimulation sequences of maximal flashes-double depolarization (see Figures 5Cb, 5E, and 6A for examples) was used to calculate the total pool size (Figure 5D). To do so, the charge transfer of mEPSCs recorded from n = 9 cells (Figure 1D; 74.8 ± 15.9 pC for time intervals of 5 ms; see also Borst and Sakmann, 1996) were used after correction for the (small) nonspecific blocking effect of 7-chloro-kynurenic acid on AMPA receptors (see above).

Equations for Ca^{2+} Saturation

According to the quantal theory of synaptic transmission (Katz, 1969), the amplitude of an evoked EPSC, Y is given by Y = p·N·q, with release probability, p; total number of readily releasable quanta, N; and quantal size, q (which can either be quantal amplitude, or quantal charge transfer in our case). We assume here that individual quanta add up linearly to give a total response, Y, and that the number of readily releasable quanta, N, is limited, either by the number of docked vesicles or by the number of a subset of docked vesicles that are competent for release.

For the first estimate of N using saturation of transmitter output with elevated $[Ca^{2+}]_e$ (Figures 1–3), we make use of the Ca^{2+} dependency of release probability, p. We assume that p is a higher order function of $[Ca^{2+}]$ at the release site, $[Ca^{2+}]_{rs}$, according to a Hill-type relationship:

$$p = p_{max} \cdot \frac{[Ca^{2+}]_{rs}^{n}}{[Ca^{2+}]_{rs}^{n} + K^{n}} \quad (1)$$

Thus, when $[Ca^{2+}]_{rs} >> K$, p should be equal to p_{max}. In general, p_{max} is not necessarily 1, since even at fully occupied Ca^{2+} sensors during an action potential, p might be limited to values < 1 by the short time of full occupancy (see Discussion).

$[Ca^{2+}]_{rs}$ was manipulated by changing the extracellular Ca^{2+} concentration, $[Ca^{2+}]_e$. For the conventional Dodge-Rahamimoff (1967) formalism, a linear relation between $[Ca^{2+}]_{rs}$ and $[Ca^{2+}]_e$ must be assumed (Reid et al., 1998). However, Ca^{2+} influx during presynaptic action potentials saturates with increasing $[Ca^{2+}]_e$ (Figure 2). A simple Michaelis-Menten saturation equation was used to fit the plot of Ca^{2+} influx, J_{Ca} versus $[Ca^{2+}]_e$:

$$J_{Ca} = J_{Ca,max} \cdot \frac{[Ca^{2+}]_e}{[Ca^{2+}]_e + EC_{50}} \quad (2)$$

with EC_{50}, the value of $[Ca^{2+}]_e$ for half-maximal Ca^{2+} influx. The low value of this parameter (2.6 mM $[Ca^{2+}]_e$) indicated a strong saturation of Ca^{2+} influx.

Release probability should be more closely related to Ca^{2+} influx, J_{Ca}, than to extacellular Ca^{2+} concentration, $[Ca^{2+}]_e$. We therefore plotted relative EPSC amplitudes, Y/Y_{2Ca}, as a function of J_{Ca} (Figure 3). This data set could be well fitted with a Hill equation of the form:

$$Y/Y_{2Ca} = Y_{max}/Y_{2Ca} \cdot \frac{J_{Ca}^{n}}{J_{Ca}^{n} + K^{n}} \quad (3)$$

in which Y_{max}/Y_{2Ca} is the expected maximal potentiation of EPSC amplitudes with respect to the value at 2 mM $[Ca^{2+}]_e$.

Acknowledgments

We would like to thank Drs. C. Rosenmund, T. Sakaba, A. Marty, and G. Borst for comments on earlier versions of the manuscript. This work was supported by a grant from Deutsche Forschungsgemeinschaft (DFG-SFB 406).

Received February 8, 1999; revised May 24, 1999.

References

Augustine, G.J., Charlton, M.P., and Smith, S.J. (1985). Calcium entry and transmitter release at voltage-clamped nerve terminals of squid. J. Physiol. *369*, 163–181.

Barnes-Davies, M., and Forsythe, I.D. (1995). Pre- and postsynaptic glutamate receptors at a giant excitatory synapse in rat auditory brainstem slices. J. Physiol. *488*, 387–406.

Borst, J.G.G., and Sakmann, B. (1996). Calcium influx and transmitter release in a fast CNS synapse. Nature *383*, 431–434.

Borst, J.G.G., and Sakmann, B. (1999). Effect of changes in action potential shape on calcium currents and transmitter release in a calyx-type synapse of the rat auditory brainstem. Phil. Trans. R. Soc. Lond. B *354*, 355–363.

Borst, J.G.G., Helmchen, F., and Sakmann, B. (1995). Pre- and postsynaptic whole-cell recordings in the medial nucleus of the trapezoid body of the rat. J. Physiol. *489*, 825–840.

Caicedo, A., and Eybalin, M. (1999). Glutamate receptor phenotypes in the auditory brainstem and mid-brain of the developing rat. Eur. J. Neurosci. *11*, 51–74.

Chuhma, N., and Ohmori, H. (1998). Postnatal development of phase-locked high-fidelity synaptic transmission in the medial nucleus of the trapezoid body of the rat. J. Neurosci. *18*, 512–520.

Church, P.J., and Stanley, E.F. (1996). Single L-type calcium channel conductance with physiological levels of calcium in chick ciliary ganglion neurons. J. Physiol. *496*, 59–68.

Delaney, K.R., and Zucker, R.S. (1990). Calcium released by photolysis of DM-nitrophen stimulates transmitter release at squid giant synapse. J. Physiol. *426*, 473–498.

Diamond, J.S., and Jahr, C.E. (1995). Asynchronous release of synaptic vesicles determines the time course of the AMPA receptor-mediated EPSC. Neuron *15*, 1097–1107.

Dittman, J.S., and Regehr, W.G. (1998). Calcium dependence and recovery kinetics of presynaptic depression at the climbing fiber to Purkinje cell synapse. J. Neurosci. *18*, 6147–6162.

Dobrunz, L.E., Huang, E.P., and Stevens, C.F. (1997). Very short-term plasticity in hippocampal synapses. Proc. Natl. Acad. Sci. USA *94*, 14843–14847.

Dodge, F.A., and Rahamimoff, R. (1967). Co-operative action of calcium ions in transmitter release at the neuromuscular junction. J. Physiol. *193*, 419–432.

Elmquist, D., and Quastel, D.M.J. (1965). A quantitative study of end-plate potentials in isolated human muscle. J. Physiol. *178*, 505–529.

Forsythe, I.D. (1994). Direct patch recording from identified presynaptic terminals mediating glutamatergic EPSCs in the rat CNS, in vitro. J. Physiol. *479*, 381–387.

Forsythe, I.D., Tsujimoto, T., Barnes-Davies, M., Cuttle, M.F., and Takahashi, T. (1998). Inactivation of presynaptic calcium current contributes to synaptic depression at a fast central synapse. Neuron *20*, 797–807.

Frankenhaeuser, B. (1957). The effect of calcium on the myelinated nerve fibre. J. Physiol. *137*, 245–260.

Geiger, J.R.P., Melcher, T., Koh, D.-S., Sakmann, B., Seeburg, P.H., Jonas, P., and Monyer, H. (1995). Relative abundance of subunit mRNAs determines gating and Ca^{2+}-permeability of AMPA receptors in principal neurons and interneurons in rat CNS. Neuron *15*, 193–204.

Grynkiewicz, G., Poenie, M., and Tsien, R. (1985). A new generation of Ca^{2+} indicators with greatly improved fluorescence properties. J. Biol. Chem. *260*, 3440–3450.

Heidelberger, R. (1998). Adenosine triphosphate and the late steps in calcium-dependent exocytosis at a ribbon synapse. J. Gen. Physiol. *111*, 225–241.

Heidelberger, R., Heinemann, C., Neher, E., and Matthews, G. (1994). Calcium dependence of the rate of exocytosis in a synaptic terminal. Nature *371*, 513–515.

Heinemann, C., Chow, R.H., Neher, E., and Zucker, R.S. (1994). Kinetics of the secretory response in bovine chromaffin cells following flash photolysis of caged Ca^{2+}. Biophys. J. *67*, 2546–2557.

Helmchen, F., Borst, J.G.G., and Sakmann, B. (1997). Calcium dynamics associated with a single action potential in a CNS presynaptic terminal. Biophys. J. *72*, 1458–1471.

Hsu, S.-F., Augustine, G.J., and Jackson, M.B. (1996). Adaptation of Ca^{2+}-triggered exocytosis in presynaptic terminals. Neuron *17*, 501–512.

Isaacson, J.S. (1998). $GABA_B$ receptor-mediated modulation of presynaptic currents and excitatory transmission at a fast central synapse. J. Neurophysiol. *80*, 1571–1576.

Jonas, P., Major, G., and Sakmann, B. (1993). Quantal components of unitary EPSCs at the mossy fibre synapse on CA3 pyramidal cells of rat hippocampus. J. Physiol. *472*, 615–663.

Kamiya, H., and Zucker, R.S. (1994). Residual Ca^{2+} and short-term synaptic plasticity. Nature *371*, 603–606.

Kaplan, J.H., and Ellis-Davies, G.C.R. (1988). Photolabile chelators for the rapid photorelease of divalent cations. Proc. Natl. Acad. Sci. USA *85*, 6571–6575.

Katz, B. (1969). The Release of Neural Transmitter Substances (Liverpool, United Kingdom: University Press).

Kemp, J.A., Foster, A.C., Leeson, P.D., Priestley, T., Tridgett, R., Iversen, L.L., and Woodruff, G.N. (1988). 7-Chlorokynurenic acid is a selective antagonist at the glycine modulatory site of the N-methyl-D-aspartate receptor complex. Proc. Natl. Acad. Sci. USA *85*, 6547–6550.

Korn, H., Triller, A., Mallet, A., and Faber, D.S. (1981). Fluctuating responses at a central synapse: n of binomial fit predicts number of stained presynaptic boutons. Science *213*, 898–901.

Kusano, K., and Landau, E.M. (1975). Depression and recovery of transmission at the squid giant synapse. J. Physiol. *245*, 13–22.

Lenn, N.J., and Reese, T.S. (1966). The fine structure of nerve endings in the nucleus of the trapezoid body and the ventral cochlear nucleus. Am. J. Anat. *118*, 375–390.

Martell, A.E., and Smith, R.M. (1974). Critical Stability Constants, Volume 1 (New York: Plenum Press).

Neher, E. (1995). The use of fura-2 for estimating Ca buffers and Ca fluxes. Neuropharmacology *34*, 1423–1442.

Neher, E. (1998). Vesicle pools and Ca^{2+}-microdomains: new tools for understanding their roles in neurotransmitter release. Neuron *20*, 389–399.

Otis, T., Zhang, S., and Trussell, L.O. (1996). Direct measurement of AMPA receptor desensitization induced by glutamatergic synaptic transmission. J. Neurosci. *16*, 7496–7504.

Partin, K.M., Patneau, D.K., and Mayer, M.L. (1994). Cyclothiazide differentially modulates desensitization of a-amino-3-hydroxy-5-methyl-4-isoxazolepropionic acid receptor splice variants. Mol. Pharmacol. *46*, 129–138.

Reid, C.A., Bekkers, J.M., and Clements, J.D. (1998). N- and P/Q-type Ca^{2+} channels mediate transmitter release with a similar cooperativity at rat hippocampal autapses. J. Neurosci. *18*, 2849–2855.

Reyes, A., Lujan, R., Rozov, A., Burnashev, N., Somogyi, P., and Sakmann, B. (1998). Target-cell-specific facilitation and depression in neocortical circuits. Nat. Neurosci. *1*, 279–285.

Rosenmund, C., and Stevens, C.F. (1996). Definition of the readily releasable pool of vesicles at hippocampal synapses. Neuron *16*, 1197–1207.

Ryugo, D.K., Wu, M.M., and Pongstaporn, T. (1996). Activity-related features of synapse morphology: a study of endbulbs of Held. J. Comp. Neurol. *365*, 141–158.

Silver, R.A., Momiyama, A., and Cull-Candy, S.G. (1998). Locus of frequency-dependent depression identified with multiple-probability fluctuation analysis at rat climbing fibre-Purkinje cell synapses. J. Physiol. *510*, 881–902.

Stevens, C.F., and Wesseling, J.F. (1998). Activity-dependent modulation of the rate at which synaptic vesicles become available to undergo exocytosis. Neuron *21*, 415–424.

Takahashi, T., Forsythe, I.D., Tsujimoto, T., Barnes-Davies, M., and Onodera, K. (1996). Presynaptic calcium current modulation by a metabotropic glutamate receptor. Science *274*, 594–597.

Takahashi, T., Kajikawa, Y., and Tsujimoto, T. (1998). G-protein-coupled modulation of presynaptic calcium currents and transmitter release by a $GABA_B$ receptor. J. Neurosci. *18*, 3138–3146.

Thomas, P., Wong, J.G., Lee, A.K., and Almers, W. (1993). A low affinity Ca^{2+} receptor controls the final steps in peptide secretion from pituitary melanotrophs. Neuron *11*, 93–104.

Trussell, L.O., Zhang, S., and Raman, I.M. (1993). Desensitization of AMPA receptors upon multiquantal neurotransmitter release. Neuron *10*, 1185–1196.

von Gersdorff, H., Schneggenburger, R., Weis, S., and Neher, E. (1997). Presynaptic depression at a calyx synapse: the small contribution of metabotropic glutamate receptors. J. Neurosci. *17*, 8137–8146.

Wang, L.-Y., and Kaczmarek, L.K. (1998). High-frequency firing helps replenish the readily releasable pool of synaptic vesicles. Nature *394*, 384–388.

Wu, L.G., Westenbroek, R.E., Borst, J.G.G., Catterall, W.A., and Sakmann, B. (1999). Calcium channel types with distinct presynaptic localization couple differentially to transmitter release in single calyx-type synapses. J. Neurosci. *19*, 726–736.

Xu, T., Naraghi, M., Kang, H., and Neher, E. (1997). Kinetic studies of Ca^{2+} binding and Ca^{2+} clearance in the cytosol of adrenal chromaffin cells. Biophys. J. *73*, 532–545.

Yamada, K.A., and Tang, C.-M. (1993). Benzothiazides inhibit rapid glutamate receptor desensitization and enhance glutamatergic synaptic currents. J. Neurosci. *13*, 3904–3915.

Zucker, R.S. (1973). Changes in the statistics of transmitter release during facilitation. J. Physiol. *229*, 787–810.

Zucker, R.S. (1996). Exocytosis: a molecular and physiological perspective. Neuron *17*, 1049–1055.